Polymer(Korea), Vol. 40, No. 5, pp. 728-735 (2016)
http://dx.doi.org/10.7317/pk.2016.40.5.728

ISSN 0379-153X(Print)
ISSN 2234-8077(Online)

전기화학적 합성방법이 폴리아닐린의 전기화학적 특성 및 모폴로지에 미치는 영향

김은옥† · 최민정

수원대학교 자연과학대학 화학과

(2016년 4월 8일 접수, 2016년 6월 1일 수정, 2016년 6월 4일 채택)

Effects of Electrodeposition Methods on Electrochemical and Morphological Properties of Polyaniline

Eunok Kim† and Minjeong Choi

Department of Chemistry, the University of Suwon, Hwaseong-si, Gyeonggi-do 18323, Korea

(Received April 8, 2016; Revised June 1, 2016; Accepted June 4, 2016)

초록: 변전위법(potentiodynamic)과 정전류법(galvanostatic)으로 polyaniline 필름을 제조하여, 전기화학적 합성방법이 필름의 전기화학적 및 구조적 특성과 모폴로지에 미치는 영향을 확인하였다. 두 합성방법은 결정성뿐만 아니라 산화상태와 도핑레벨의 차이를 유발하였다. 또한 필름의 모폴로지는 서로 다른 성장과정에도 영향을 받았다. 변전위법으로 제조된 필름의 경우, layer-by-layer 성장을 통해 매끄럽고 균일한 모폴로지를 나타낸다. 반면에 정전류법으로 제조된 필름은 분해로 인해 거칠어진 모폴로지를 나타낸다. 변전위법과 정전류법으로 제조한 필름의 거칠기(R_q)는 각각 94와 171 nm, 전도도는 2.74와 0.98 S/cm이다.

Abstract: Polyaniline (PAni) films were electrodeposited in the potentiodynamic and galvanostatic modes, and the effects of the deposition methods on the electrochemical, structural, and morphological properties of the films are discussed. The two deposition methods resulted in different degrees of oxidation and doping degrees as well as film crystallinities. Furthermore, the morphologies of the films were affected by the different growth processes. In the case of the PAni film deposited in the potentiodynamic mode, a smoother and more homogeneous morphology was observed owing to the layer-by-layer growth of the film. On the other hand, in the case of the PAni film deposited in the galvanostatic mode, a rougher surface morphology was observed owing to the degradation process. The root-mean-square roughness values of the films deposited in the potentiodynamic and galvanostatic modes were 94 and 171 nm, respectively, while their conductivities were 2.74 and 0.98 S/cm, respectively.

Keywords: polyaniline, potentiodynamic, galvanostatic, electrodeposition.

Introduction

Conducting polymers have attracted considerable interest owing to their high electrical conductivities and good environmental stabilities, as well as the ease of preparation. Polypyrrole, polyaniline (PAni), and polythiophene are the most widely studied conducting polymers. Among these polymers, PAni has emerged as a promising candidate with significant potential for use in various applications, including in light-emitting diodes, transparent electrodes, and gas and humidity sensors, as well as for the electromagnetic radiation and corrosion protection of metals.[1] Conducting polymers are preferentially prepared by electropolymerization, which is a popular and general method, because of its simplicity and reproducibility. Furthermore, it requires only a single-compartment cell.[2] The morphology of electrodeposited PAni films depends significantly on deposition parameters, such as the concentration of the monomer, type of protonic acid used, pH of the resultant solution, deposition time and temperature, and applied current.[3]

The polymerization of aniline involves the insertion of chloride anions as a dopant in HCl, which is used as the electrolyte. The process can be expressed as follows:

†To whom correspondence should be addressed.
E-mail: eokim@suwon.ac.kr

$$(PAni)_n + nyCl^- \rightarrow [PAni^{y+}(Cl^-)_y]_n + nye^-$$

Here, y refers to the doping degree (ratio of the number of protonated polaronic emeraldine to the number of unprotonated aniline monomers).[4] On the application of potential, oligomers are generated at the interface between the electrode and the electrolyte solution; these grow to a critical chain length, at which they become insoluble in the electrolytic solution. Consequently, they precipitate on the electrode surface and produce nuclei, which continue to grow, yielding a polymeric layer.[5]

The properties of PAni films are typically affected by deposition methods (i.e., potentiodynamic, potentiostatic, and galvanostatic). PAni films prepared using the potentiodynamic mode (PDM) exhibit a surface morphology different from those of the film prepared in the potentiostatic and galvanostatic modes (GSM). During potentiodynamic deposition, the potential is swept between low and high potentials in cycles, resulting in layer-by-layer deposition, with each layer becoming electrically active before the next one is deposited. On the other hand, during galvanostatic deposition, the current can be controlled. Hence, the deposition rate of these films can be controlled with greater accuracy.[6]

The aim of this study is to investigate the effects of the deposition method used on the electrochemical, structural, and morphological properties of PAni films. The fabricated PAni are characterized by cyclic voltammetry (CV), chronopotentiometry (CP), Fourier transform infrared (FTIR) and UV-Visible spectroscopy (UV-Vis), scanning electron microscopy (SEM), atomic force microscopy (AFM), X-ray diffraction (XRD), and the 4-point probe method.

Experimental

Materials. Aniline (≥99.0%, Duksan Pure Chemicals) was purified by double distillation before use. Hydrochloric acid (HCl, 37.0%, Duksan Pure Chemicals) and dimethyl sulfoxide (DMSO, ≥99.0%, Sigma-Aldrich) were used as received. All the aqueous solutions were prepared using deionized water (>18.2 MΩ).

Electrochemical Polymerization. The electrochemical experiments were performed in a one-compartment three-electrode electrochemical cell. Aniline was used in a concentration of 0.3 M in an electrolyte solution of 1.5 M HCl. N_2 gas was flushed to remove the oxygen present during the preparation of the electrolyte solution. The deposition area of the working electrode, indium tin oxide (ITO, 9.55 Ω/cm^2), was 0.25 cm^2. A platinum plate (1.0 cm×1.5 cm) and a Ag/AgCl (3 M NaCl) electrode were used as the counter and reference electrodes, respectively. The surface of the ITO electrode was cleaned by sonication for 20 min in ethanol, followed by careful rinsing with distilled water and ethanol in sequence. The electropolymerization of aniline was performed either by CV using a sweep rate of 10 mV/s for 20 cycles between 0.0 and 1.1 V or by CP for 80 min at a current density of 2.4 mA/cm^2. The experiments were conducted at 273 K. The HCl doped PAni (PAni-salt) was dedoped using sodium hydroxide to obtain the emeraldine base (PAni-EB). The PAni films were dried in a vacuum oven at 50 °C for 24 h.

Characterization. The electrochemical experiments were performed using a WBCS 3000 battery cycler (WonATech). The polymer structures of the films were investigated using FTIR. FTIR spectra was recorded on an FTIR/ATR 4100 spectrometer (Jasco) in the attenuated total reflection mode for wavenumbers of 600-1600 cm^{-1}. UV-Vis spectra was recorded on an S-3100 Spectrophotometer (Scinco) over the wavelengths of 250-1100 nm using DMSO as the solvent. Since SEM only provides visual data related to the morphologies of the films, AFM was also employed to obtain more detailed morphological information. AFM is better for investigating the surface morphologies to obtain their roughness values. In particular, AFM can provides two dimensional (2-D) and three dimensional (3-D) images of the film surfaces.[7] The films were rinsed with methanol and coated with Pt prior to the SEM imaging of their surfaces. The SEM images were recorded at 15 kV using an MAIA 3 (Tescan) system. Further, 2-D and 3-D AFM images were acquired using an NX 10 (Park Systems) system operating in the non-contact mode. Etched silicon tips were employed for the morphology evaluations. In order to avoid artifacts from the tips, each experiment was performed using a new tip. X-ray diffraction (XRD) was performed using a D2 Phaser (Bruker) diffractometer with Cu-Kα radiation (λ= 0.154 nm) at 40 kV and 40 mA. The scan range (2θ) was 16°-30°. The thicknesses of the films were measured using a micrometer caliper, while their sheet resistances and conductivities were measured by the 4-point probe technique using a 2401 source measurement unit (Keithley).

Results and Discussion

Figure 1 shows the CV curves obtained during the polymerization of aniline. After the 1st cycle, film growth is con-

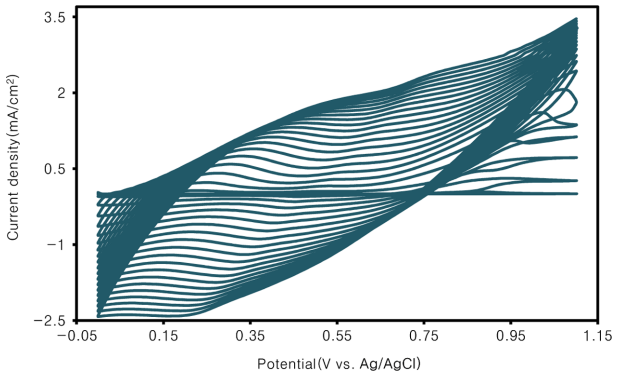

Figure 1. Cyclic voltammetry curves obtained during the growth of PAni films.

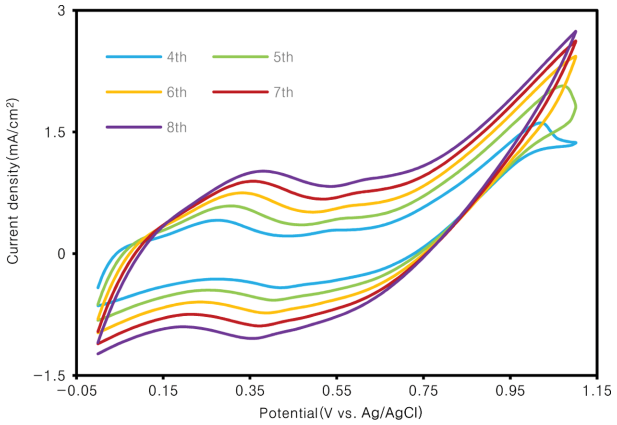

Figure 2. Cyclic voltammetry curves for PAni films for the 4th to 8th cycles.

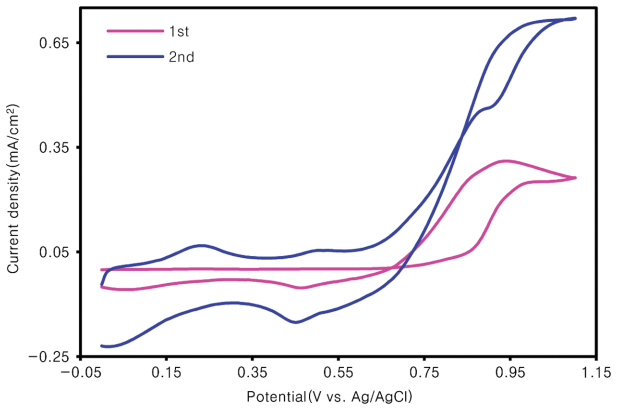

Figure 3. Cyclic voltammetry curves for PAni films for the 1st and 2nd cycles.

trolled by the autocatalytic polymerization of aniline throughout the subsequent cycles.[8] The oxidation and reduction peaks are shifted in the positive and negative directions, respectively. The shifts in these peaks are consistent with the ohmic contribution to the overpotential behavior, which is attributed to the internal resistance of the electrode.[8-10] Figure 2 shows the CV curves corresponding to the 4th to 8th cycles. Stable cycling was achieved after continuous potential sweeps for a few cycles.[11] A typical CV curve of PAni exhibits two sets of peaks related to redox reactions; these are accompanied by charge transfer and mass transport.[12] The first redox couple is associated with the conversion of the leucoemeraldine form into the polaronic emeraldine form.[13,14] The positive charge on the aniline units in the polaronic emeraldine form is balanced by a negatively charged anion.[1] In order to compensate for the charge of PAni, anion transfer from the electrolyte solution, that is, doping, is necessary.[15] The second redox couple is related to the conversion of the polaronic emeraldine form into the pernigraniline form.[13] However, in the case of thick films, the doping/dedoping of the anions is not reversible, as the anions inserted within the polymer get trapped in the polymer matrix (Figure 1).[16] Moreover, if the overall reaction is not mass transport, then sluggish electron transfer controls the kinetics.[17] With an increase in the number of cycles, the oxidation peak disappears. Further, the corresponding reduction peak is not observed in the reverse sweep. This behavior is characteristic of an irreversible process.[18]

Figure 3 shows the CV curves for the first two cycles. During the 1st anodic sweep, the current for the oxidation of the aniline monomers began to increase at 0.85 V; this is considered to be the rate-determining step. During the reverse sweep, at 1.1 V, the current still continued to increase in the cathodic sweep; this is mainly attributes to the increase in the electrode surface area because of film formation. The maximum current was observed at approximately 0.94 V, followed by the sharp decrease in current; this sharp decrease is caused by a decrease in the reaction kinetics, owing to the low potential region.[19,20] Polarons, which were generated during the 1st cycle, undergo a coupling reaction in order to produce dimers.[21] As the dimer exhibits higher conjugation than the monomer, it is oxidized more readily (see the 2nd cycle).[22]

In the GSM, the current flow in the working electrode remains constant. This deposition method allows for the film thickness to be controlled by adjusting the duration of the polymerization. Galvanostatic deposition requires an appropriate selection of current density values.[23] Figure 4 shows the CP curves obtained during the growth of PAni films: the curves corresponding to various current densities of 1.4, 1.6, 1.7, 2.0, and 2.3 mA/cm^2 are shown in the inset. As a stable CP curve is obtained for a current density of 1.7 mA/cm^2, this cur-

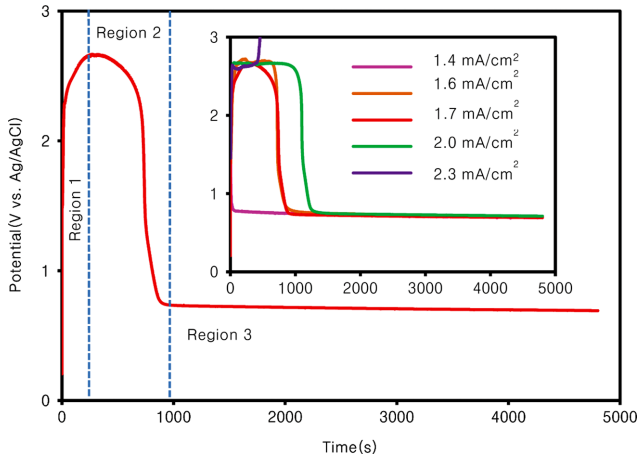

Figure 4. Chronopotentiometry curves obtained during the growth of PAni films. Inset shows the chronopotentiograms obtained at different current densities.

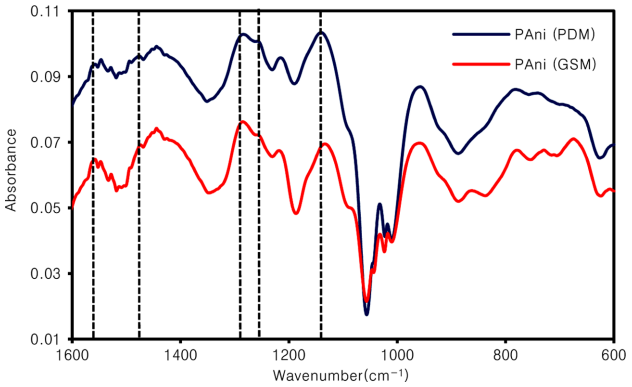

Figure 5. FTIR spectra of PAni films prepared by potentiodynamic and galvanostatic modes.

rent density is selected in further experiments. Polymerization consists of three steps. The first step indicates an overshoot in the potential from 0.21 to 2.67 V during the first few minutes; this is probably indicative of the difficulty in forming dimers and oligomers.[24,25] Also, this result implies two opposite effects: an increase of the polymerization rate and the enhancement of degradation process.[26] Once PAni was formed and degradation process was enhanced, the potential decreased from 2.67 to 0.70 V in the second step; this decrease is attributed to the fact that the potential required for the oxidation of the already formed film is less than that of the aniline monomer. In the last step, after the surface of the ITO was completely covered with a PAni film, polymerization proceeded at a nearly constant potential of 0.70 V.[23,26] This suggests that there is competition between polymerization and degradation process, which occurs at approximately the same rates.[26]

Figure 5 shows the FTIR spectra of the PAni films prepared by PDM and GSM, which are similar to each other. Peaks observed at 1563 and 1475 cm^{-1} in the spectra are assigned to the stretching vibrations of the quinone (*Q*) and benzene (*B*) rings, respectively. The presence of these two peaks clearly shows that the polymer is composed of amine and imine units.[27] The intensity ratio of these two peaks (I_Q /I_B) can be used to estimate the degree of oxidation of PAni. The intensity ratios for the films prepared under PDM and GSM are 0.966 and 0.922, respectively, suggesting that the degree of oxidation of PAni formed by PDM is greater than that formed by GSM. A peak observed at 1284 cm^{-1}, attributes to the stretching of C-N bonds in secondary aromatic amines and the delocalization of π electrons, induced by the doping of the polymer. Another peak is observed at 1256 cm^{-1}, indicative of the electrically conductive form of PAni-salt.[28] This peak is ascribable to the stretching of the C-N^{+}· polaron structure, which is generated by doping. The doping degree of the film prepared by PDM is possibly greater than that of GSM, as demonstrated by the ratio between the intensity of the peak at 1257 cm^{-1}, which assigned to the polaron structure, to that of the peak at 1284 cm^{-1}, which assigned to the delocalization of π electrons.

The intensity ratio for the film grown by PDM is greater than that of GSM. Moreover, peaks observed at 1135-1140 cm^{-1} is attributes to the vibration of the -NH^{+}= structure, which is also generated by doping. In the case of the film deposited by PDM, the peak intensity is greater at 1140 cm^{-1}. Once again, this result demonstrates a higher doping degree for the film deposited by PDM. The region between 700 and 900 cm^{-1} corresponds to deformation of aromatic rings and out-of-plane vibration of C-H bonds.[29,30] These FTIR spectra demonstrate that, in the film prepared potentiodynamically, the degree of oxidation and doping degree are greater than those in the film prepared galvanostatically.

Figure 6 shows the UV-Vis spectra of PAni-EB and PAni obtained under PDM and GSM. The spectra of PAni-EB shows two absorption peaks, at ~360 and ~630 nm. The first peak at ~360 nm is due to π-π* transition associated with the π electrons in the benzene ring which mainly a function of intrachain interaction. The second peak at ~630 nm is assigned to the excitation of an electron from the highest occupied molecular orbital (HOMO) of the benzene ring to the lowest unoccupied molecular orbital (LUMO) of the quinone ring. This peak reflects both intra- and interchain interactions.[11] As an additional electronic state was formed by doping, the PAni-

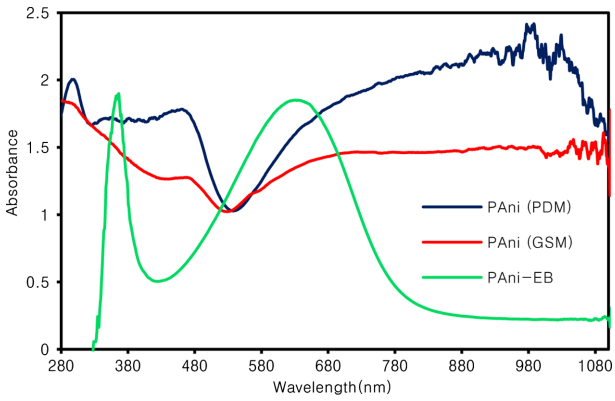

Figure 6. UV-Vis spectra of PAni-EB and PAni prepared by potentiodynamic and galvanostatic mode.

salt exhibits a different spectra from that of PAni-EB.[31] The PAni-salt exhibited three characteristic peaks: at ~300 nm, attributed to π-π* transition, and two polaron peaks at ~460 and ~820 nm in the visible region, which are attributes to the polaron-π* and π-polaron transitions (Figure 6), respectively.[20] According to Abdiryim *et al*., the doping degree can be roughly estimated from the ratio of absorbances at ~820 nm (π-polaron) and ~300 nm (π-π*).[32] Based on this ratio, it is further confirmed that PAni prepared by PDM exhibits a higher doping degree. Results obtained from UV-Vis spectra indicate that the doping degree is affected by the deposition method. Moreover, the results obtained from the UV-Vis spectra are in agreement with FTIR results, confirming that the doping degree of the PAni prepared potentiodynamically is higher than that prepared galvanostatically.

The morphologies of the PAni films are analyzed by SEM and AFM. Figure 7 shows the SEM images of the PAni films prepared by (a) PDM and (b) GSM. In both cases, fibril-like morphologies are observed to be intrinsic for the PAni film deposited on ITO.[33] According to Kemp *et al*., fibril formation occurs in three stages. First, nucleation occurs on the ITO surface; this is followed by horizontal growth to form a compact 2-D layer. Finally, vertical growth occurs, which extends the fibrils in the vertical direction.[34] As confirms in Figure 7(a), a smoother and more homogeneous morphology is observed, whereas some aggregates along the fibrils are observed in Figure 7(b). As the layer-by-layer growth occurs in the case of the film deposited by PDM, fresh nucleation during each cycle is likely to produce a discontinuous phase.[35,36] Thus, intermediates, which are formed during degradation process, could be released or terminates polymer growth.[37] Further, these intermediates could be trapped within the PAni film because of its

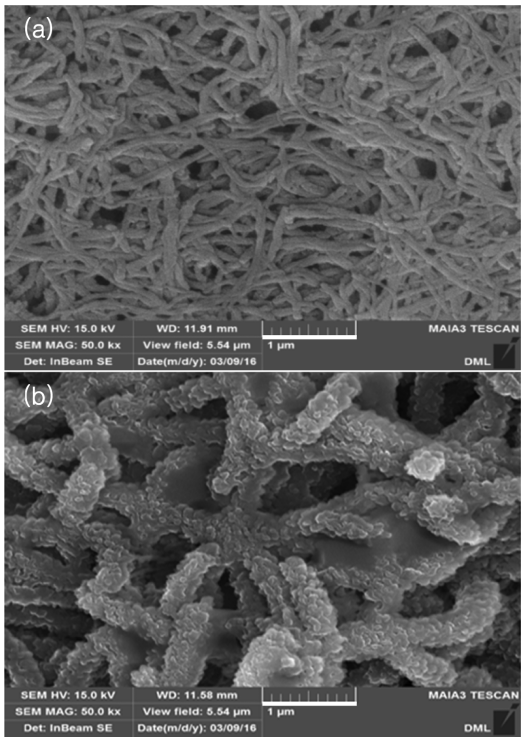

Figure 7. SEM images of PAni films prepared by (a) potentiodynamic; (b) galvanostatic modes.

continuous growth.[38] Irregularities observed along the fibrils in the form of aggregates in the film prepared by GSM are caused by polymer degradation process.[39]

Figure 8 shows the AFM images of the PAni films prepared by (a) PDM and (b) GSM. The root-mean-square roughness (R_q) values of the films prepared by PDM and GSM are 94 and 171 nm, respectively. The surface of the film prepared by PDM is significantly smoother with fewer intermediates, resulting in a more stable film.[37] On the other hand, the higher R_q value of film grown by GSM is attributed to the aggregation of polymer chains.[40] These aggregates on the surface are probably caused by the overgrowth of the chains.[41] Hence, the surface of the film prepared galvanostatically is rougher and less homogeneous as compared with that prepared potentiodynamically, due to its aggregates.

The PAni structure was evaluated by XRD, in order to investigating the crystallinity and ordering of the polymer chains. Figure 9 shows XRD patterns of the PAni films prepared by PDM and GSM. The patterns of PAni exhibit three peaks superimposed on a broad scattering background, indicating that chains are partially crystalline.[42] These three peaks are observed at 2θ of 16.3° (d=5.43 Å), 21.1° (d=4.21 Å), and 25.3° (d=3.52 Å), respectively. The first peak is indicative of

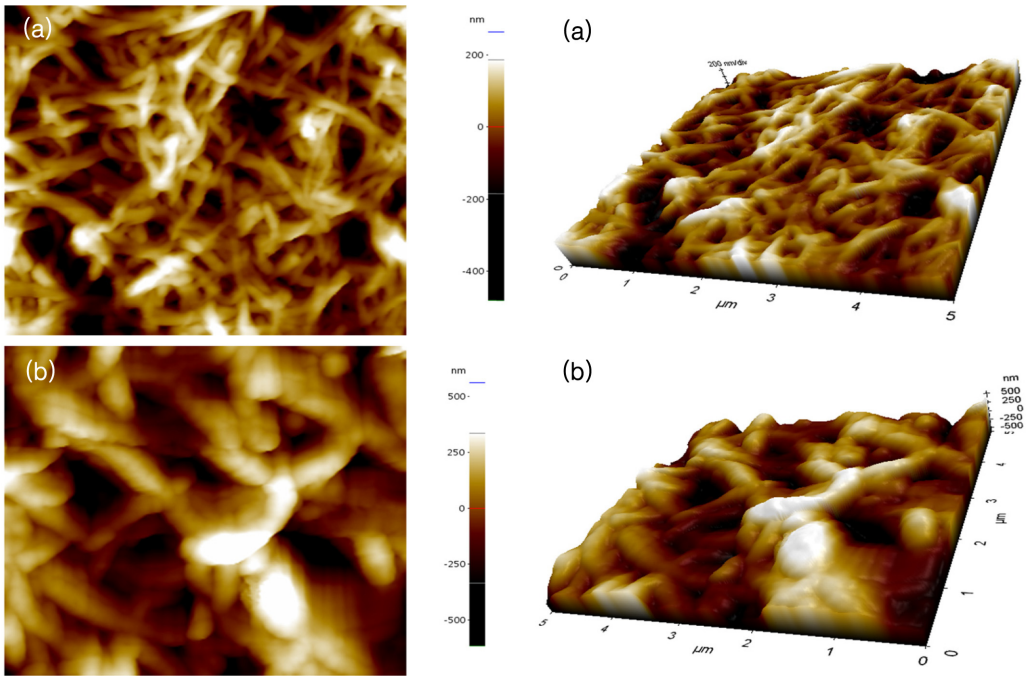

Figure 8. AFM images of PAni prepared by (a) potentiodynamic; (b) galvanostatic modes.

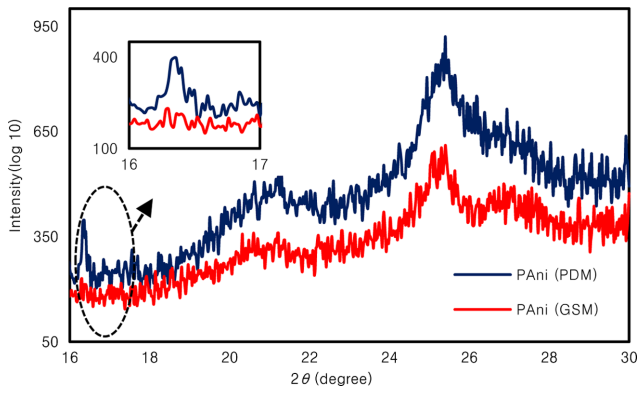

Figure 9. XRD patterns of PAni prepared by potentiodynamic and galvanostatic modes.

intrachain ordering within the polymer chains.[43] The film prepared under PDM exhibits a strong and sharp peak at 16.3°, which implies that the film has an ordered structure in contrast to the film prepared under GSM. This result is probably attributed to the periodic interruption in the growth of the polymer: thus, the polymer chains have time to rearrange themselves during potentiodynamic polymerization. The second peak is attributed to periodicity parallel to the backbone chain; it also represents the characteristic distance between the ring planes of benzene rings in adjacent chains or close-contact interchain distance.[32] The last peak is attributed to periodicity perpendicular to the backbone chain; it also corresponds to the face-to-face interchain stacking distance between phenyl rings. Thus, the increase in the intensity of this peak along with the decrease in background intensity implies improved π-π interchain stacking, which suggests a more planar chain conformation with reduced torsion angles between the phenyl rings and the ring planes of the backbone.[42] In short, the XRD patterns reveal that the intra- and interchains are more ordered in the PAni film prepared potentiodynamically.

The sheet resistances are 12.58 and 35.01 Ω/sq and the conductivities are 2.74 and 0.98 S/cm for the PAni films grown by PDM and GSM, respectively. The structural changes induced by doping affects its conductivity: this can be explained on the basis of the different degrees of oxidation as well as doping degrees of PAni.[13] For the films prepared under PDM, the increase in conductivity is caused by a higher degree of oxidation and doping degree as compared with that of GSM.[44] Typically, degradation process is associated with the shortening of the chain length, which yields irregularities and a more resistive skeleton in the polymer. Consequently, when degradation process occurs, conductivity decreases.[45] The irregularities on the surface of the film prepared under GSM adversely affects conductivity.[46] PAni is reported to consist of ordered crystalline regions in an amorphous medium. The ordered regions are the primary factors responsible for elec-

trical conductivity.[43] The higher ordered structure in the film prepared under PDM, which was characterized by XRD, results in higher electrical conductivity. As a result, it can be concluded that the conductivity of PAni is affected by various factors, including its degree of oxidation, doping degree, morphology, as well as the crystallinity of the PAni. On account of its growth process, the PAni film prepared galvanostatically exhibits a lower conductivity.

Conclusions

In this study, the effects of the deposition methods (potentiodynamic and galvanostatic) on the electrochemical, structural, and morphological properties of PAni are discussed. The PAni exhibits different degrees of oxidation as well as doping degree, which is higher under potentiodynamic deposition. The polymerization of aniline is determined to be irreversible, as confirmed by the CV curves, which also exhibits autocatalytic polymerization and overpotential behavior. When degradation process is enhanced, the potential decreases in CP curve. As a result, the PAni film prepared galvanostatically exhibits aggregates on the surface. The surface roughness of the film prepared potentiodynamically is higher than that prepared galvanostatically. The different deposition methods also affect the ordering of the polymer chains. The film grown potentiodynamically exhibits a highly ordered crystalline structure as compared with that grown galvanostatically. The conductivity is lower for the film prepared under galvanostatic condition. These results are confirmed that the degree of oxidation and doping degree as well as the crystallinity of the PAni prepared galvanostatically are lower and that its surface is rough.

Acknowledgement: This study is partially supported by ‘SaJeDongHang’ program at the center for teaching and learning of the University of Suwon. The authors would like to thank Mr. Ewan Lee (Park Systems Inc.) for assistance with the AFM experiments and for useful discussions related to image analysis. They also thank Jieun Lee for assistance with the electrochemical experiments.

References

1. M. Alam, A. A. Ansari, M. R. Shaik, and N. M. Alandis, *Arabian J. Chem.*, **6**, 341 (2013).
2. P. A. Savale, D. J. Shirale, K. Datta, P. Ghosh, and M. D. Shirsat, *Int. J. Electrochem. Sci.*, **2**, 595 (2007).
3. D. S. Dhawale, R. R. Salunkhe, V. S. Jamadade, T. P. Gujar, and C. D. Lokhande, *Appl. Surf. Sci.*, **255**, 8213 (2009).
4. N. Popović, B. Z. Jugović, B. Jokić, Z. Knežević-Jugovć, J. S. Stevanović, B. N. Grgur, and M. M. Gvozdenović, *Int. J. Electrochem. Sci.*, **10**, 1208 (2015).
5. M. A. del Valle, M. Romero, F. R. Díaz, F. Armijo, R. del Río, I. Núñez, and E. A. Dalchiele, *Int. J. Electrochem. Sci.*, **8**, 12321 (2013).
6. R. Balint, N. J. Cassidy, and S. H. Cartmell, *Acta Biomater.*, **10**, 2341 (2014).
7. P. Paik and K. K. Kar, *Surf. Eng.*, **24**, 341 (2008).
8. G. Das and H. H. Yoon, *Int. J. Nanomedicine*, **10**, 55 (2015).
9. Q. Z. Dong, L. Y. Zhu, H. S. Wan, C. C. Guo, and G. Yu, *Int. J. Electrochem. Sci.*, **9**, 8024 (2014).
10. W. Lin, K. Xu, J. Peng, Y. Xing, S. Gao, Y. Ren, and M. Chen, *J. Mater. Chem. A*, **3**, 8438 (2015).
11. D. Yang, W. Lu, R. Goering, and B. R. Mattes, *Synth. Met.*, **159**, 666 (2009).
12. M. Vuki, M. Kalaji, L. Nyholm, and L. M. Peter, *J. Electroanal. Chem.*, **332**, 315 (1992).
13. E. Song and J.-W. Choi, *Nanomaterials*, **3**, 498 (2013).
14. D.-W. Wang, F. Li, J. Zhao, W. Ren, Z.-G. Chen, J. Tan, Z.-S. Wu, I. Gentle, G. Q. Lu, and H.-M. Cheng, *ACS Nano*, **3**, 1745 (2009).
15. A. Baba, S. Tian, F. Stefani, C. Xia, Z. Wang, R. C. Advincula, D. Johannsmann, and W. Knoll, *J. Electroanal. Chem.*, **562**, 95 (2004).
16. S.-J. Choi and S.-M. Park, *J. Electrochem. Soc.*, **149**, 26 (2002).
17. A. Mallik and B. C. Ray, *Int. J. Electrochem.*, **2011**, 16 (2011).
18. M. Gu, J. Zhang, Y. Li, L. Jiang, and J.-J. Zhu, *Talanta*, **80**, 246 (2009).
19. E. C. Venancio, C. A. R. Costa, S. A. S. Machado, and A. J. Motheo, *Electrochem. Commun.*, **3**, 229 (2001).
20. K. M. Molapo, P. M. Ndangili, R. F. Ajayi, G. Mbambisa, S. M. Mailu, N. Njomo, M. Masikini, P. Baker, and E. I. Iwuoha, *Int. J. Electrochem. Sci.*, **7**, 11859 (2012).
21. C. Yang, J. Du, Q. Peng, R. Qiao, W. Chen, C. Xu, Z. Shuai, and M. Gao, *J. Phys. Chem. B*, **113**, 5052 (2009).
22. J. Heinze, B. A. Frontana-Uribe, and S. Ludwigs, *Chem. Rev.*, **110**, 4724 (2010).
23. M. Gvozdenović, B. Jugović, J. Stevanović, and B. Grgur, *Hem. Ind.*, **68**, 673 (2014).
24. X. Du, Y. Xu, L. Xiong, Y. Bai, J. Zhu, and S. Mao, *J. Appl. Polym. Sci.*, **131**, 40827 (2014).
25. P. D. Gaikwad, D. J. Shirale, P. A. Savale, K. Datta, P. Ghosh, A. J. Pathan, G. Rabbani, and M. D. Shirsat, *Int. J. Electrochem. Sci.*, **2**, 488 (2007).
26. D. Sazou, M. Kourouzidou, and E. Pavlidou, *Electrochim. Acta*, **52**, 4385 (2007).
27. M. V. Kulkarni and A. K. Viswanath, *Eur. Polym. J.*, **40**, 379 (2004).
28. M. Trchová and J. Stejskal, *Pure Appl. Chem.*, **83**, 1803 (2011).
29. E. C. Gomes and M. A. S. Oliveira, *Am. J. Polym. Sci.*, **2**, 5 (2012).

30. A. M. Pharhad-Hussain and A. Kumar, *Bull. Mater. Sci.*, **26**, 329 (2003).
31. V. J. Babu, S. Vempati, and S. Ramakrishna, *Mater. Sci. Appl.*, **4**, 1 (2013).
32. T. Abdiryim, Z. Xiao-Gang, and R. Jamal, *Mater. Chem. Phys.*, **90**, 367 (2005).
33. C. Dhand, M. Das, G. Sumana, A. K. Srivastava, M. K. Pandey, C. G. Kim, M. Datta, and B. D. Malhotra, *Nanoscale*, **2**, 747 (2010).
34. N. T. Kemp, J. W. Cochrane, and R. Newbury, *Synth. Met.*, **159**, 435 (2009).
35. K. R. Prasad and N. Munichandraiah, *J. Electrochem. Soc*., **149**, 1393 (2002).
36. L. Cheng and S. Dong, *Electrochem. Commun*., **1**, 159 (1999).
37. S.-J. Choi and S.-M. Park, *Adv. Mater.*, **12**, 1547 (2000).
38. S. K. Mondal, K. R. Prasad, and N. Munichandraiah, *Synth. Met*., **148**, 275 (2005).
39. C. Q. Cui, X. H. Su, and J. Y. Lee, *Polym. Degrad. Stab*., **41**, 69 (1993).
40. M. N. Khalid, S. Yasin, and M. R. Khan, *Turk. J. Phys.*, **28**, 271 (2004).
41. A. D. Jagadale, V. S. Kumbhar, R. N. Bulakhe, and C. D. Lokhande, *Energy*, **64**, 234 (2014).
42. K. H. Lee, S. U. Cho, S. H. Park, A. J. Heeger, C.-W. Lee, and S.-H. Lee, *Nature*, **441**, 65 (2006).
43 S. J. Varma, F. Xavier, S. Varghese, and S. Jayalekshmi, *Polym. Int*., **61**, 743 (2012).
44. Z. Zakaria, N. F. A. Halim, M. H. V. Schleusingen, A. K. M. S. Islam, U. Hashim, and M. N. Ahmad, *J. Nanomater.*, **2015**, 6 (2015).
45. M. J. Bleda-Martínez, C. Peng, S. Zhang, G. Z. Chen, E. Morallón, and D. Cazorla-Amorós, *J. Electrochem. Soc.*, **155**, 672 (2008).
46. S. Tawde, D. Mukesh, and J. V. Yakhmi, *Synth. Met*., **125**, 401 (2002).